Supplementary Information

In vivo micro computed tomography detection and decrease in amyloid load by using multifunctionalized gold nanorods: a neurotheranostic platform for Alzheimer s disease

Francisco Morales-Zavala, [a,b,c] Pedro Jara-Guajardo, [a,b] David Chamorro, [d,e] Ana L. Riveros, [a,b] America Chandia-Cristi, [d,e] Nicole Salgado, [f] Paola Pismante, [g] Ernest Giralt, [h,i] Macarena Sánchez-Navarro, [h] Eyleen Araya, [j] Rodrigo Vasquez, [a,j] Gerardo Acosta, [k] Fernando Albericio, [k,l] Alejandra Alvarez,*[d,e] and Marcelo J. Kogan.*[a,b]

[a] Departamento de Química Farmacológica y Toxicológica, Facultad de Ciencias Químicas y Farmacéuticas, Universidad de Chile, Santiago, Chile.
[b] Advanced Center for Chronic Diseases (ACCDiS), Sergio Livingstone 1007, Independencia, Santiago, Chile.
[c] Centro de Nanotecnología Aplicada, Facultad de Ciencias, Universidad Mayor, Camino La Piramide 5750, Huechuraba, Chile
[d] Facultad de Ciencias Biológicas, Pontificia Universidad Católica de Chile, Alameda 340, Santiago 8331010, Chile.
[e] Centro de envejecimiento y regeneración (CARE), Facultad de Ciencias Biológicas, Pontificia Universidad Católica de Chile, Santiago, Chile.
[f] Unidad de Microscopía Avanzada, Facultad de Ciencias Biológicas, Pontificia Universidad Católica de Chile, Santiago, Chile.
[g] Departamento de Tecnologías Nucleares, División de Investigación y Aplicaciones Nucleares, Comisión Chilena de Energía Nuclear.
[h] Institute for Research in Biomedicine (IRB Barcelona), Barcelona Institute of Science and Technology (BIST), Baldiri Reixac 10, Barcelona, 08028, Spain.
[i] Department of Inorganic and Organic Chemistry, University of Barcelona, Martí I Franqués 1-11, Barcelona, 08028, Spain.
[j] Departamento de Ciencias Químicas, Facultad de Ciencias Exactas, Universidad Andrés Bello, Santiago, Chile.
[k] CIBER-BBN, Networking Centre on Bioengineering, Biomaterials and Nanomedicine & Department of Organic Chemistry, Marti i Franques 1-11, University of Barcelona (UB), 08028 Barcelona, Spain.
[l] School of Chemistry & Physics, University of KwaZulu-Natal, Durban 4001, South Africa.

*Corresponding author, mkogan@ciq.uchile.cl & aalvarez@bio.puc.cl

List of contents:

1- *Quantification of GNRs*

2- *In vitro human BBB cellular model*

3- *Detection of GNRs-D1/Ang2 in mouse brain APPswe/PSEN1dE9 by STEM dark-field*

4- *Detection of GNRs-D1/Ang2 in mouse brain APPswe/PSEN1dE9 by gold enhancement protocol*

Supplementary Results

1- *GNRs-D1/Ang2 characterization*

Supplementary table

Table S1*. Summary of the transversal and longitudinal hydrodynamic diameters (Dh) and Z potentials (pZ) of GNRs-CTAB, conjugated to PEG, Ang2, D1 and D1/Ang2.*

Supplementary figures

S1. *Characterization of the nanosystems*

S2. *TEM micrographs*

S3. *Histological identification of GNRs-D1/Ang2 in the brain cortex*

S4. *Emission spectrum of GNRs tagged with Alexa Fluor 647 and conjugated to Peg, D1, Ang2 and D1/Ang2*

S5. *Percentage of the dose of gold that reaches the liver*

S6. *Images of the skull by micro-CT of a transgenic APPswe/PSEN1dE9 mouse (TG) treated with a single dose of 100 µL of GNRs-PEG*

S7. *Images of the skull by micro-CT of a WT animal (C57bl/6) without treatment*

S8. *Images of the skull by micro-CT of a wt C57bl/6 mouse treated with a single dose of 100 µL of GNRs-PEG*

Supplementary Materials and methods

1- *Quantification of GNRs*

The samples were sealed by friction welding and exposed for 17 h to a neutron flux of 0.25–1.3 n/cm^{2}s with a power of 5 mW, using a RECH-1 reactor at the CCHEN, thereby triggering the conversion of ^{197}Au to ^{198}Au. After 7–12 days of neutron bombardment, the γ -rays emitted by the samples were counted and sorted by energies using a germanium detector coupled to a PC-based multichannel γ-ray spectrometer. The γ ray-spectra were analyzed using the software GENIE 2000 Canberra. Gold standards were run with the experimental samples to standardize a gold element data library from which the amount of gold present in the unknown samples was calculated. Given that detection limits by neutron activation can be influenced by the elemental composition of the sample, background levels were determined by irradiating the untreated tissue samples (controls) of a similar size and composition to that of the experimental samples.

The final uncertainty was evaluated by combining the individual components with those contributed by neutron activation: μ-weight of the sample, μ-weight of the standard reference material, μ-measure of the analyte in the sample, μ-measure of the analyte in the standard, μ-neutron flux of the standard reference material, μ-neutron flux of the sample, and μ correction of the dead time in the sample and in the standard reference material. The uncertainty informed corresponds to the expanded uncertainty (U), which was calculated with a cover factor equal to 2. This factor is equivalent to a level of confidence of 95%.

With the gold concentration (CAu) data and the length and width averages of the GNRs determined by TEM, the GNR concentration (nanomolar) was determined as follows[1]:

$$\text{Concentration of } GNRs = \frac{4 \times C\text{Au}}{\rho\text{Au} \times \pi \times \text{W} \times 2\text{L}}$$

Where ρAu is the density of gold atoms in the bulk (59 atoms/nm^3), CAu is the gold concentration (nM) determined by gold neutron activation, W is the width (nm) of the GNRs determined by STEM and L is the length (nm) of the GNRs determined by STEM.

2- *In vitro human BBB cellular model*

Permeability experiments were performed using the model developed in Prof. R. Cecchelli's laboratory.[2] Briefly, endothelial cells derived from pluripotent stem cells and bovine pericytes were thawed in gelatin-coated Petri dishes (Corning). Pericytes were cultured in DMEM pH 6.8 and endothelial cells were cultured in supplemented endothelial cell growth medium (sECM) (Sciencell Research Laboratories). After 48 h, endothelial cells were seeded in 12-well Transwell inserts (8000 cell/well) and pericytes were plated in 12-well plates (50000 cells/well), previously coated with Matrigel and gelatin, respectively. The sECM medium was used for both cell lines and changed every 2-3 days. The assays were performed 7-8 days after seeding by placing the endothelial cells into new wells without pericytes. To perform the assay, 500 µL of the GNRs solution (0.05 nM) in Ringer HEPES was added to the donor compartment and 1500 µL of Ringer HEPES were added to the acceptor compartment. Lucifer Yellow (25 µM) was added as a control of barrier integrity (Papp < $15 \cdot 10^{-6}$ cm/s). The plates were incubated for 2 h at 37 °C, and the solutions from both compartments were recovered and analyzed. The samples were evaluated in triplicates. The amount of gold was quantified using an ICP-MS and the apparent permeability was calculated using the following formula:

$$Papp = (t) \cdot VDt \cdot A \cdot QD(t0)$$

where *Papp* is obtained in cm/s, Q(t) is the amount of compound at time *t* in the acceptor well, VDt is the volume in the donor well, *t* is the time of the experiment time in seconds, *A*

is the area of the membrane in cm and *QD(t0)* is the amount of compound in the donor compartment at the beginning of the experiment.

3- *Detection of GNRs-D1/Ang2 in mouse brain APPswe/PSEN1dE9 by STEM dark-field*

The brain was then extracted from the animal (see section in the manuscript) and the hippocampus was isolated and fixed by immersion with a 1% solution of osmium tetroxide for 1 hour. Subsequently, the hippocampus was washed 3 times in sodium phosphate buffer for 10 minutes and then the sample was dehydrated in ethanol following the sequence: 30% -50% -70% -90% and -96%; 7 minutes in each step, then washed twice in absolute ethanol and 2 more times with acetone and then infiltrated with Epon resin for 2 days, embedded in the same resin, polymerized at 70 °C for 48 h. 1 µm sections (Ultramicrotome Sorvall Porter Blum) were stained with 1% toluidine blue in 1% sodium borate to find a fine-cut area. Ultra-thin slices of 60 nm were obtained using the same ultra-microtome, and then mounted on Cu grates coated with Formvar. Finally, the samples were stained with 2% uranyl acetate in water and lead citrate. Subsequently, micrographs were obtained by FEG-SEM (Inspect F50, FEI), with a STEM detector (dark-field).

4- *Detection of GNRs-D1/Ang2 in APPswe/PSEN1dE9 mouse brain by the gold enhancement protocol*

FFPE Tissue processing for histology and special stains.

Whole brain samples were fixed for 24 hours on 4 %PFA and then processed for paraffin embedding. Sagittal sections of 15 um were cut from each paraffin block, and sections were then dried, deparaffinized and re-hydrated on distilled water. Gold Enhancement was

performed with the Nanoprobes GoldEnhance TM LM Kit, according to the manufacturer's instructions. Once this procedure was finished, the same sections were stained for amyloid deposits with Congo Red stain and nuclear contrast was performed with Mayer's Hematoxylin. Images of the stained slides were taken with an ICC50W Camera on a DM500 Leica Microscope, with 100x magnification.

Supplementary Results

1- GNRs-D1/Ang2 characterization

The GNRs produced here showed similar characteristics to the GNRs previously described (Morales-Zavala *et al*.). The DLS characterization shows that the GNRs have a transversal hydrodynamic diameter near 4 nm and a longitudinal hydrodynamic diameter near 68 nm. The GNRs showed a zeta potential of -11 mV and rod-shape nanostructure, with an aspect ratio (length/width) of approximately 4 (Supporting Material, TEM images). In the Uv-Vis-Nir spectra of GNRs-D1/Ang2, we observed two characteristic peaks of absorption at 510 nm and 760 nm for the transversal and longitudinal plasmons, respectively. The number of peptides per nanoparticle was determined by amino acid analysis and corresponded to 423 ± 23 molecules of D1 and 173 ± 36 molecules of Ang2. The information corresponding to the characterization of the nanosystems used on this work is detailed in **Table S1, Figures S1 and S4**.

	Dh (nm)		
	Transversal	Longitudinal	pZ (mV)
GNRs-CTAB	2 ± 0.1	46 ± 1	55 ± 2
GNRs-PEGs	4 ± 0.2	56 ± 2	-23 ± 3
GNRs-Ang2	5 ± 0.1	62 ± 2	-17 ± 1
GNRs-D1	5 ± 0.1	62 ± 1	-7 ± 6
GNRs-D1/Ang2	4 ± 0.2	68 ± 6	-11 ± 1

Table S2. Summary of the transversal and longitudinal hydrodynamic diameters (Dh) and Z potentials (pZ) of GNRs-CTAB, conjugated to PEG, Ang2, D1 and D1/Ang2.

A

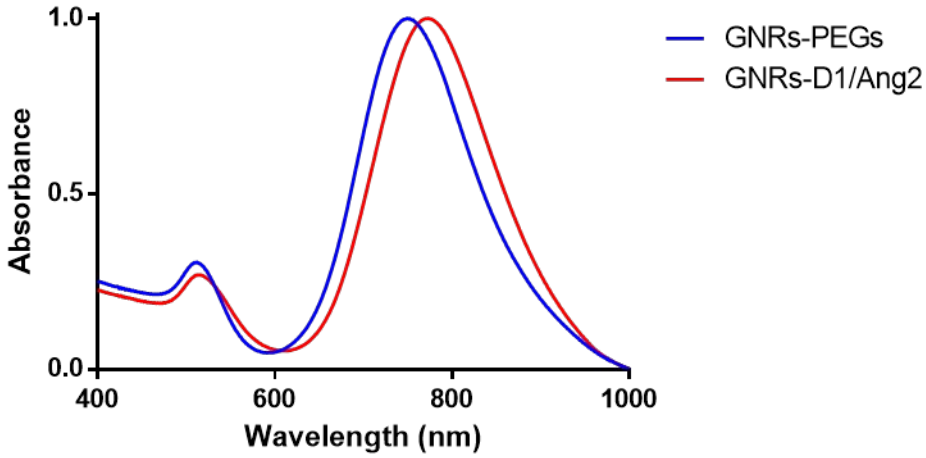

B

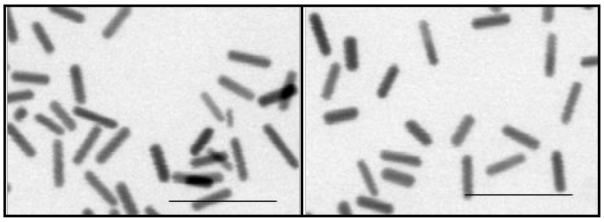

C

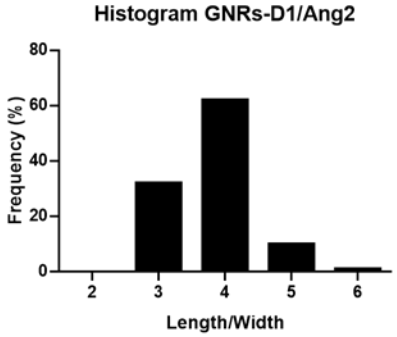

Figure S1:Characterization of the nanosystems. A) Uv-Visible spectrum of GNRs-PEGs and GNRs-D1/Ang2. B) STEM image set for GNRs-PEGs (left) GNR-D1/Ang2 (right) (bar = 500 nm). C) Histogram distribution indicating Length/Width of GNRs-D1/Ang2.

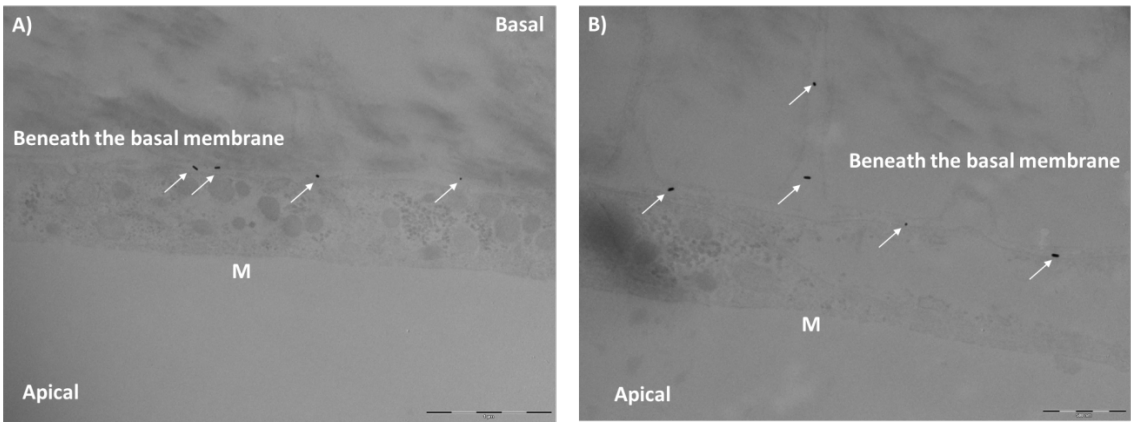

Figure S2. TEM micrographs. Panels show that (A) GNRs-Ang2 and (B) GNRs-D1/Ang2 are able to cross the endothelial cells and accumulate underneath the basal membrane. Scale bar: 1 µm (A), 500 nm (B).

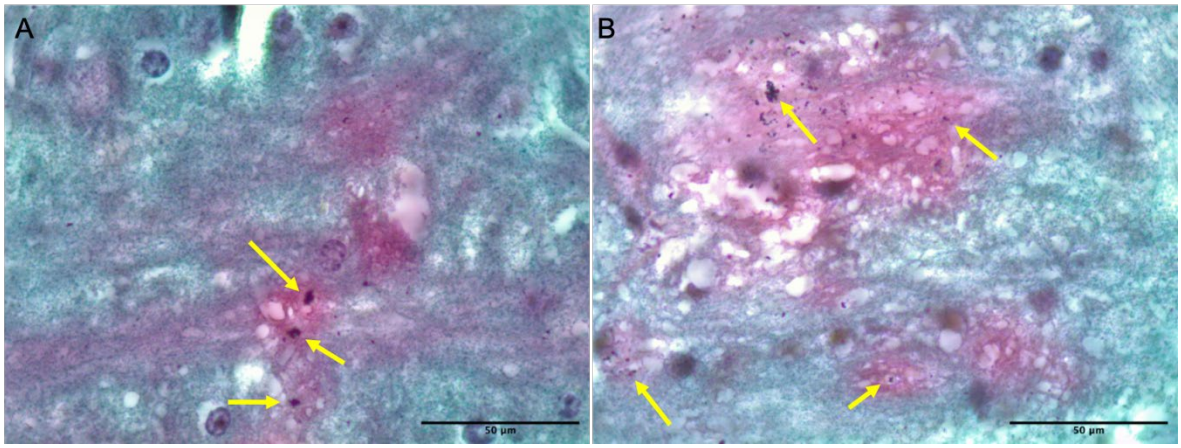

Figure S3. Histological identification of GNRs-D1/Ang2 in the brain cortex. (A, B) Representative optical microscopy images of brain slices obtained 15 min after APPswe/PSEN1ΔE9 mice were injected (i.v.) with GNRs-D1/Ang2 [10 nM]. The yellow arrows indicate the GNRs-D1/Ang2 localized at the amyloid plaque stained Congo Red (red arrow).

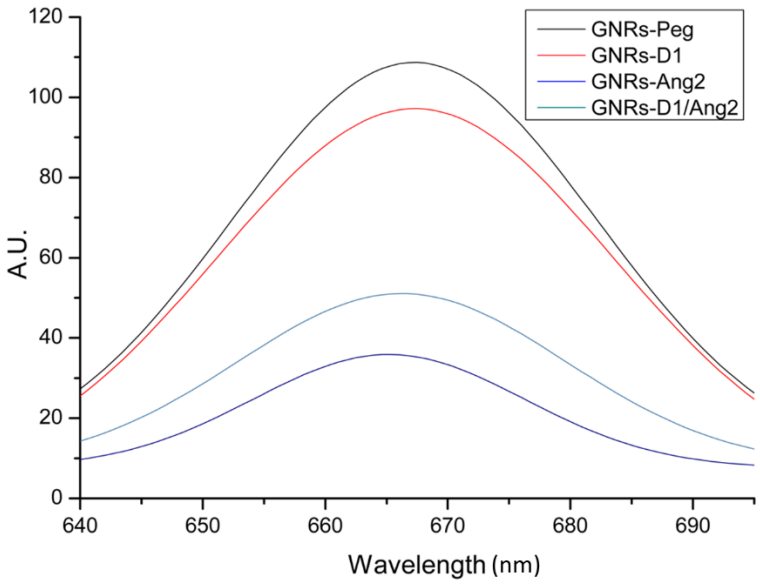

Figure S4. Emission spectrum of GNRs tagged with Alexa Fluor 647 and conjugated to Peg, D1, Ang2 and D1/Ang2.

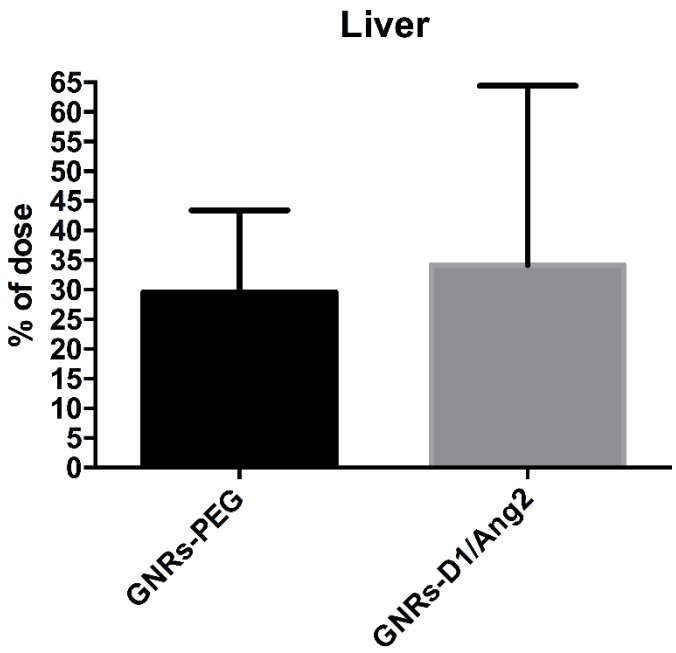

Figure S5. Percentage of the dose of gold that reaches the liver. 100 ul [10 nM] of the nanoparticles were injected into the tail vein of transgenic APPswe/PSEN1dE9 mice (TG) (n=4). The animals were sacrificed at 15 minutes. The quantification of gold was performed by neutron activation.

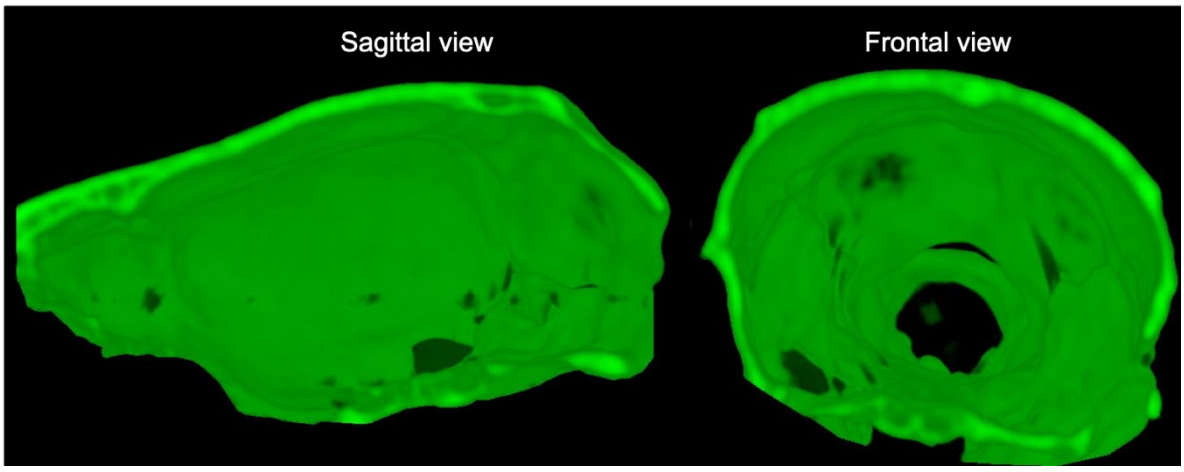

Figure S6. Images of the skull by micro-CT of a transgenic APPswe/PSEN1dE9 mouse (TG) treated with a single dose of 100 µL of GNRs-PEG.

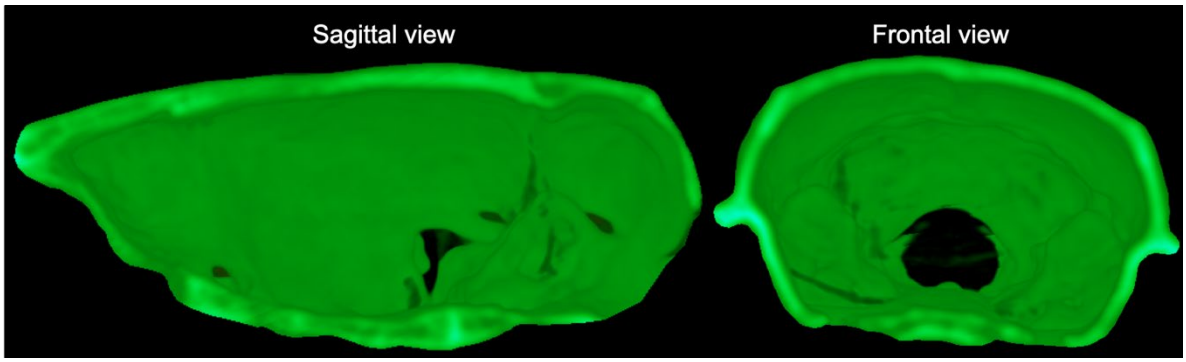

Figure S7. Images of the skull by micro-CT of a wt C57bl/6 mouse treated with a single dose of 100 µL of GNRs-PEG.

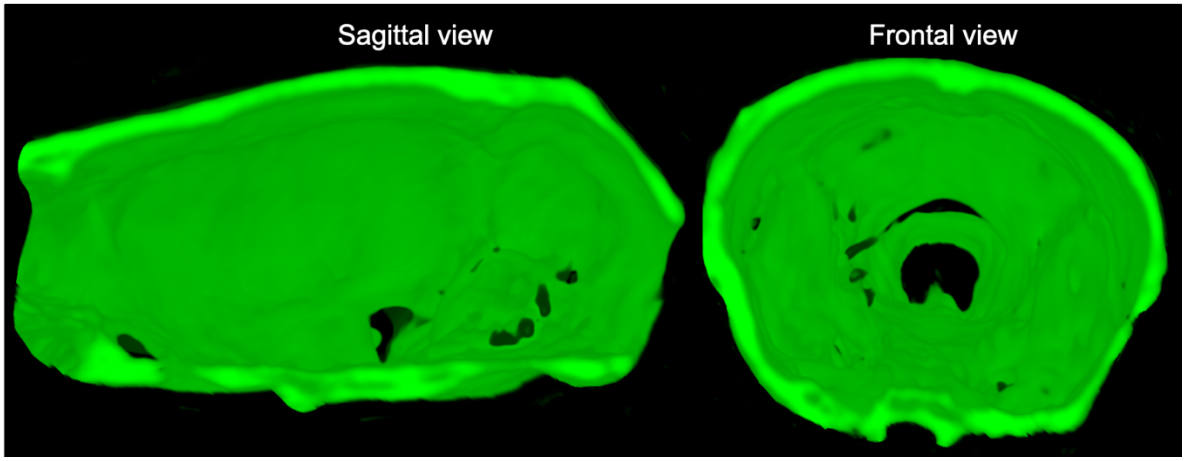

Figure S8. Images of the skull by micro-CT of a WT animal (C57bl/6) without treatment.

References:

1. S. Link and M. A. El-Sayed, *Annual Review of Physical Chemistry*, 2003, **54**, 331-366.
2. R. Cecchelli, S. Aday, E. Sevin, C. Almeida, M. Culot, L. Dehouck, C. Coisne, B. Engelhardt, M.-P. Dehouck and L. Ferreira, *PLOS ONE*, 2014, **9**, e99733.